Proposal for direct air capture of CO_2 during the Antarctic winter using physisorption

Clifford W. Hicks[1, 2, *]

[1] *School of Physics and Astronomy, University of Birmingham, Birmingham B15 2TT, United Kingdom*
[2] *Max Planck Institute for Chemical Physics of Solids, Nöthnitzewr Str. 40, 01187 Dresden, Germany*

The possibility of direct air capture of CO_2 in Antarctica is discussed. Because the concentration of H_2O in the atmosphere during the Antarctic winter is extremely low, an installation for direct air capture could employ a physisorption-based process, allowing, in principle, a very short adsorption/desorption cycle time. The lower required binding allows more options for materials for the sorbent. With a shorter cycle time, more resource could be spent on structuring the sorbent to improve energy efficiency, for example by improving its mass efficiency if desorption is driven thermally.

1. Introduction. At present humanity emits ≈ 35 Gt/y (gigatonnes per year) of CO_2 [1]. Direct capture of CO_2 from the environment is likely to become a necessary component of climate change mitigation [2, 3]. The companies Climeworks [4] and Carbon Engineering [5], for example, are pursuing direct air capture (DAC) of CO_2 through installations built for this purpose. The required area for these installations is much less than that required for biochar or enhanced weathering, other possible methods for CO_2 capture. However, the energy requirement is vast. Both companies employ and adsorption/desorption cycle to capture CO_2. Carbon Engineering's process uses a KOH sorbent, and is calculated to consume 390 kJ per mole of captured CO_2 (4.0 eV per CO_2 molecule) [5]. Climeworks' process employs amine scrubbing, and also requires, as of 2015, ≈ 400 kJ/mol [6, 7]. Scaled up to a capture rate of 10 Gt/y, 4 eV per molecule equates to $9 \cdot 10^{19}$ J/y, roughly matching the primary energy consumption of the United States. Energy efficiency is critical for implementing DAC at scale.

This article explores the possibility of performing DAC in Antarctica. Its central premise is that a physisorption-based process can be employed. Physisorption is adsorption through interaction with the electrical properties of the adsorbate molecules: van der Waals and electrostatic interactions. In the CO_2 molecule, the oxygen atoms are negatively charged and the carbon positively charged, so CO_2 molecules adhere to charged surfaces more strongly than the other major components of the atmosphere, except H_2O. H_2O, having a strong electric dipole moment, usually adheres to charged surfaces even more strongly. Therefore, to obtain CO_2 rather than H_2O, adsorption processes operated in temperate climates must typically use chemisorption, which is adsorption involving exchange of an electron and which offers chemical selectivity [8–10].

During the Antarctic winter the concentration of H_2O in the atmosphere is low enough that chemical selectivity might not be necessary. For pure physisorption there is no activation energy. In addition, during the Antarctic winter there will be no fluid layer on the sorbent surface through which CO_2 must diffuse [3]. Therefore, the cycle time can in principle be very short. A short cycle time, in turn, would allow more resource to be spent on structuring the sorbent, which in turn could yield substantial improvement in energy efficiency. For example, if desorption is driven by heating, then energy efficiency is improved by making the sorbent as light as possible relative to its capacity to adsorb CO_2.

There are three further advantages to operation in Antarctica. One is the reliability of the katabatic winds, a potential power source. The second is that the high plateau of the Antarctic ice sheet is empty; there are no competing land uses, and the penguins live on the coast. The third is that captured CO_2 could be stored by injection into the ice sheet.

The following sections are: (2) The capture cycle and energy consumption are summarised. (3) A conceptual sorbent structure suitable for a 1 s cycle time is presented. 1 s is chosen as an illustration what may be possible, not as a carefully-considered optimum. (4) The optimum adsorption binding energy is calculated. (5) The energy cost of purge cycles to remove H_2O is discussed. (6) The katabatic winds and (7) storage of captured CO_2 are discussed.

2. Operating conditions and the capture cycle. The capture installations are presumed to operate on the high plateau of the east Antarctic ice sheet, at an elevation of around 3500 m, where the ambient pressure is ≈ 65 kPa. The average winter temperature is below -60°C (213 K), and can drop to -90° C [11]. An ambient CO_2 concentration of 400 ppm is assumed.

The capture cycle is summarised in Table I. A maximum operating temperature for the capture machinery

TABLE I. The capture cycle.

1.	Adsorb CO_2 at $T \leq -58$° C, $P \approx 65$ kPa.
2.	Desorb CO_2 at $T \approx 100$° C, $P = 1.3$ kPa.
3.	Compress the CO_2 to ~ 10 MPa, while allowing it to cool to -40° C.
4.	Inject the CO_2 into the ice sheet.

of −58° C is selected, allowing it to operate for slightly more than half of the year [11]. This limit is due to the presence of H_2O in the atmosphere. CO_2 is adsorbed at ambient conditions, and then is desorbed by reducing the pressure and heating the sorbent to ≈ 100° C. The pressure reduction reduces the amount of heating required, and so also the energy consumption for desorption [6, 7]. In step 3, the CO_2 is then compressed to ≈ 10 MPa, and as it is compressed heat sinks allow it to cool to ≈ −40° C. The CO_2 will liquify. For storage, it can then be injected into the ice sheet; at a pressure of 10 MPa it can be injected to a depth of 1 km.

Table II lists the components of the energy consumption that will be discussed. These figures assume a sorbent capacity of 10 wt % CO_2, meaning that the mass of CO_2 captured when every binding site is occupied is 10% of the mass of the empty sorbent.

3. Illustrative sorbent structure. To obtain an illustrative cycle time of 1 s, which is 3–4 orders of magnitude faster than typical [3], I suppose that the adsorption and desorption times will each be ∼0.3 s, leaving ∼0.4 s to carry out the temperature and pressure changes. In reality, the optimum cycle time will be set by a balance between the economic cost of the sorbent, which favours a short cycle time, and limits on the mechanical engineering required to drive the temperature and pressure swing, which will almost certainly favour a longer cycle time. This is because, for energy efficiency, the amount of material that undergoes cyclic heating must be kept to a minimum. The rate at which CO_2 can be delivered to the sorbent is essentially fixed by the energy budget for driving the flow through the sorbent, so the amount of CO_2 that could be captured in each cycle is proportional to the cycle time, $t_{\rm cycle}$. The depth that heat penetrates into surfaces is proportional to $\sqrt{t_{\rm cycle}}$, so the energy cost of cyclic heating per captured CO_2 molecule will in general be proportional to $1/\sqrt{t_{\rm cycle}}$: smaller for longer $t_{\rm cycle}$. As illustrated in the conceptual sorbent structure shown in Fig. 1, if the sorbent support structure is conductive then heating could be accomplished by running current through the sorbent; it is nevertheless inevitable that some of the applied heat will spread beyond the sorbent.

To minimise conduction of heat beyond the sorbent, it will be advantageous to hold the sorbent with thermally insulating supports. That would mean that the heat of adsorption dissipates into the airflow. This is acceptable. It will be shown below that the optimum adsorption binding energy is ∼ 0.4 eV, so the temperature of the airflow rises by:

$$\Delta T = \frac{0.4\ \text{eV} \times 4 \cdot 10^{-4}}{\frac{5}{2} k_{\rm B}} = 0.7\ \text{K}.$$

TABLE II. Energy consumption for the conceptual process discussed in this paper, in eV per molecule of captured CO_2. A sorbent capacity of 10 wt % CO_2 is assumed.

0.4 eV	driving the airflow through the sorbent
0.4 eV	adsorption energy
0.6 eV	heating the sorbent (extrinsic component)
0.4 eV	purging H_2O
0.2 eV	compressing the captured CO_2 to ∼ 10 MPa

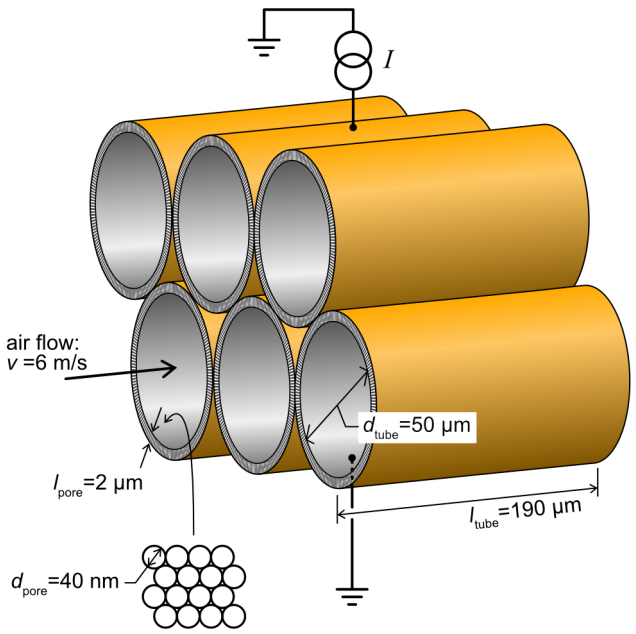

FIG. 1. Conceptual sorbent structure for an adsorption time of ∼ 0.3 s. It consists of a set of tubes of diameter $d_{\rm tube}$ = 50 μm through which air passes, lined with pores of diameter $d_{\rm pore}$ = 40 nm and depth $l_{\rm pore}$ = 2 μm. The tube shells may be conductive, so that the sorbent could be heated by applying current.

In our illustrative structure (Fig. 1), the sorption sites are inside pores of diameter $d_{\rm pore}$ and length $l_{\rm pore}$. The pores are on the inside of larger tubes, of inner diameter $d_{\rm tube}$ and length $l_{\rm tube}$, through which air is flushed.

The Reynolds number for flow through a tube is ${\rm Re} = \rho v d_{\rm tube}/\mu$, where ρ is the density of the air, v the average flow velocity through the tube, and μ the dynamic viscosity of the air. At 65 kPa and 213 K, $\rho \approx 1.1$ kg/m^3. $\mu \approx 1.4 \cdot 10^{-5}$ kg/m-s at 213 K [12], and I select $d_{\rm tube} = 50$ μm. Setting $v = 6$ m/s, as indicated in Fig. 1, yields Re ≈ 25, so laminar flow is expected [13]. For laminar flow through a tube [13],

$$v = \frac{\Delta P d_{\rm tube}^2}{32 l_{\rm tube} \mu}, \qquad (1)$$

where ΔP is the pressure differential across the tube.

In setting the tube dimensions, we require that CO_2 molecules be able to diffuse across the tube diameter in the time that the flow transits the tube. At time t', the typical diffusion velocity is $v_{\rm diff} = \sqrt{D/t'}$, where D is

the diffusion constant of CO_2 in air at 65 kPa and $T \approx$ 200 K. The average diffusion velocity between $t' = 0$ and $t' = t$ is $\langle v_{\rm diff} \rangle = 2\sqrt{D/t}$. The condition that molecules have time to diffuse across the tube diameter corresponds to $\langle v_{\rm diff} \rangle = v d_{\rm tube}/l_{\rm tube}$. Setting t to the transit time, $l_{\rm tube}/v$, yields:

$$v = \frac{4 l_{\rm tube} D}{d_{\rm tube}^2}. \quad (2)$$

Combining Eqs. 1 and 2 yields:

$$v = \sqrt{\frac{D \Delta P}{8\mu}}. \quad (3)$$

ΔP is obtained by selecting the power consumption for driving the flow. If this power consumption is set at 0.4 eV per captured CO_2 molecule, the fans driving the flow are 50% efficient, and the total capture efficiency for CO_2 passing through the device is 75% (Carbon Engineering's target [5]), then ΔP = 200 Pa. $D \approx 1.2 \cdot 10^{-5}$ m^2/s [12], yielding v = 6 m/s. For comparison, the inflow rate selected by Carbon Engineering is 1.4 m/s [5].

$d_{\rm tube}$ does not enter Eq. 3, so $d_{\rm tube}$ = 50 μm is a somewhat arbitrary choice. Applying Eq. 1 with $d_{\rm tube}$ = 50 μm yields $l_{\rm tube}$ = 190 μm.

The pore dimensions ($d_{\rm pore}$ = 40 nm and $l_{\rm pore}$ = 2 μm) are discussed further in the Appendix. Here I provide two salient facts. (1) The capture site density on the pore surface is taken to be one per (4.3 Å)^2, approximately the capture site density reported for TiO_2(110) [14] and Fe_2O_4(001) [15]. With these pore specifications, $d_{\rm tube}$ = 50 μm, and v = 6 m/s, it takes 0.3 s for enough CO_2 to pass through the sorbent to fill the capture sites. (2) The characteristic time for diffusion into and out of the pores is $\sim$ 0.03 s, so the capture rate is not limited by diffusion into the pores.

4. Energy consumption for dry air. In this section, the optimum adsorptive binding energy $E_{\rm ad}$ is calculated under an assumption that there is no H_2O in the atmosphere. A major factor in this calculation is the extrinsic energy cost to run the adsorption/desorption cycle: the energy that must be expended independently of the amount of CO_2 actually captured, for example in heating sorbent material other than the binding sites themselves. When the extrinsic energy consumption is low, energy efficiency is maximised when $E_{\rm ad}$ is relatively low, such that the occupation swing (the binding site occupation after the adsorption phase minus that after the desorption phase) is well below 100% [16]. When the extrinsic energy consumption is substantial, the occupation swing should be large.

The desorption pressure is set here to 2% of the ambient pressure: 1.3 kPa. This is, again, a value chosen for illustration, not a carefully-considered optimum. The occupation swing is calculated using the Langmuir model for adsorption: the density of binding sites is fixed, the rate of adsorption is proportional to the number of unoccupied sites, and binding is characterised by a single binding energy, $E_{\rm ad}$, that is independent of the number of adjacent sites that are occupied. Let n be the actual density of adsorbed CO_2 molecules on the pore surfaces. The probability that an incoming CO_2 molecule adsorbs is taken to be $S \times (1 - n/n_{\rm sat})$, where S is the sticking fraction and $n_{\rm sat} = (4.3\ \text{Å})^{-2}$. S is set to 0.75, the value reported for gases impacting a TiO_2(110) surface at 32 K [17]. Let $r_{\rm att}$ be the attempt rate for desorption and $r_{\rm in}$ be the impact rate of CO_2 molecules on the sorbent surface. In equilibrium, the rate of escape equals the capture rate:

$$r_{\rm att} n \exp\left(-\frac{E_{\rm ad}}{k_{\rm B} T}\right) = \left(1 - \frac{n}{n_{\rm sat}}\right) S r_{\rm in}. \quad (4)$$

For $r_{\rm att}$, a quantum-limited rate is taken: $r_{\rm att} = k_{\rm B}T/\hbar$, which evaluates to $2.8 \cdot 10^{13}$ s^{-1} at 213 K. $r_{\rm in}$ is calculated from the pressure of the gas: $P = \frac{2}{3} m v_{\rm molec} I$, where I is the impact rate and m is the mass of the dominant molecule. For the adsorption phase, rearranging this expression and taking into account the concentration of CO_2 and its slightly slower velocity yields:

$$r_{\rm in} = \frac{3}{2} \frac{4 \cdot 10^{-4}}{\sqrt{m_{\rm air} m_{\rm CO2}}} \frac{65\ \text{kPa}}{v_{\rm molec}(T)}. \quad (5)$$

Taking $m_{\rm air}$ = 29 g/mol and $v_{\rm molec} = (3 k_{\rm B} T/m_{\rm air})^{1/2}$ = 430 m/s, $r_{\rm in} = 1.5 \cdot 10^{24}$ m^{-2}s^{-1} at 213 K. For the desorption phase, the gas is taken to be pure CO_2:

$$r_{\rm in} = \frac{3}{2 m_{\rm CO2}} \frac{1.3\ \text{kPa}}{v_{\rm CO2}(T)}. \quad (6)$$

The desorption temperature $T_{\rm de}$ is calculated as a function of $E_{\rm ad}$ and the adsorption temperature, $T_{\rm ad}$, which is equal to the ambient temperature. The energy required for desorption is taken to be $E_{\rm ad}$ for each molecule that is captured in the adsorption phase and released in the desorption phase, plus the energy required to heat the sorbent from $T_{\rm ad}$ to $T_{\rm de}$; I assume that there is no mechanism for recovering this heat. The sorbent is taken to have a heat capacity of 683 J/kg-K, which is the heat capacity of TiO_2 at room temperature [18]. Results are calculated for two sorbent capacities: 5 wt % CO_2 and 10 wt % CO_2. For silica aerogel functionalised with amine groups, capacities of up to $\approx$ 10 wt % have been demonstrated in atmospheres of 400 ppm CO_2 [19–21].

The criterion for $T_{\rm de}$ is that the captured CO_2 escapes the pores in $\sim$ 0.3 s. Because the diffusion time out of the pores is $\sim$ 0.03 s, this condition corresponds to a requirement that 10% of the adsorbed CO_2 molecules desorb instantly: if the pores were blocked so that no CO_2 could escape, 10% of the CO_2 molecules would desorb.

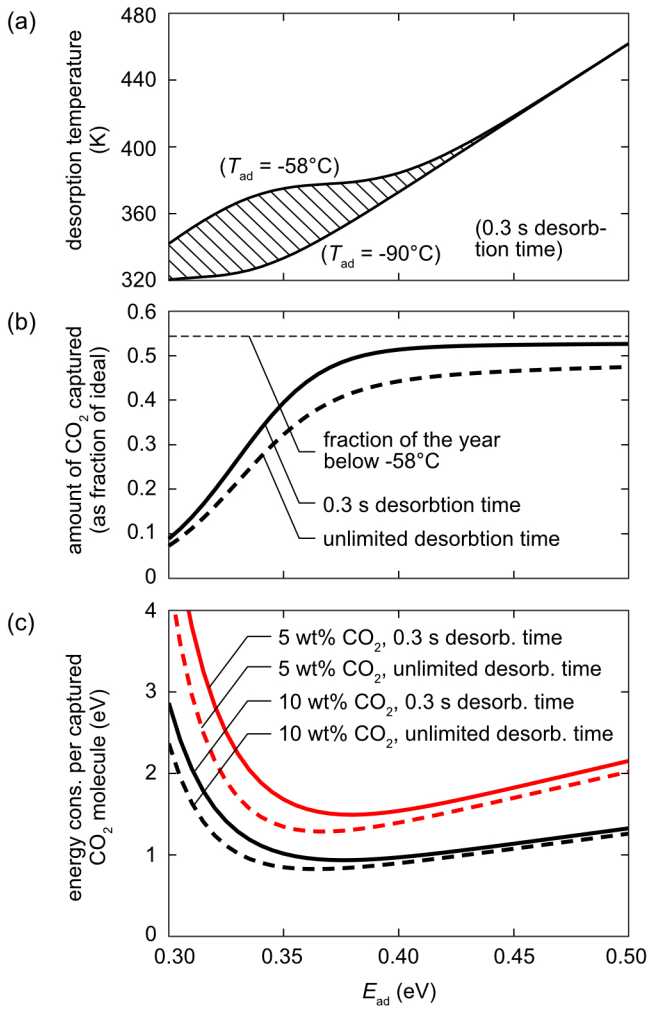

FIG. 2. (a) Desorption temperature range for $T_{\rm ad}$ between $-90°$ C and $-58°$ C, under a requirement that captured CO_2 molecules escape the pores in ~ 0.3 s. (b) The amount of CO_2 captured over the course of the year as a fraction of a hypothetical maximum in which the occupation swing is 100% and the capture machinery operates year-round. (c) Energy consumption for heating the sorbent per captured CO_2 molecule, and for two possible sorbent capacities. Results in panels (b) and (c) are averaged over the observed temperature distribution at the Vostok research station [11], with a cutoff temperature of $-58°$ C.

Results are shown in Fig. 2. Fig. 2(a) shows the range of desorption temperatures for $T_{\rm ad}$ between $-90°$ C and $-58°$ C, as a function of $E_{\rm ad}$. Fig. 2(b) shows the amount of CO_2 captured as a fraction of a hypothetical maximum in which the occupation swing is 100% and the capture machinery operates year-round. For high $E_{\rm ad}$, this fraction saturates at the fraction of the year there the temperature is below $-58°$ C. Finally, Fig. 2(c) shows the average energy consumption per captured CO_2 molecule. The results in Figs. 2(b) and (c) are averaged over the temperature distribution at the Vostok station [11], with a $-58°$ C cutoff.

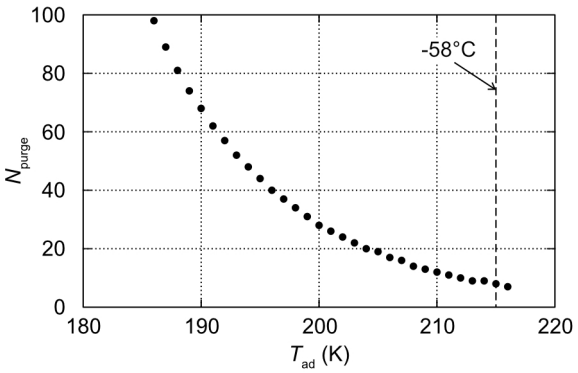

FIG. 3. Optimum purge period as a function of $T_{\rm ad}$. Every $N_{\rm purge}{}^{\rm th}$ desorption cycle is run at an elevated temperature to drive off H_2O, at an assumed energy cost of four times that for a regular desorption cycle.

Energy efficiency is maximised for $E_{\rm ad}$ between 0.35 and 0.40 eV. For a sorbent capacity of 10 wt % CO_2, the energy consumption is about 1.0 eV per molecule, which can be divided into two parts: an intrinsic component, ≈ 0.4 eV, to drive the desorption, and an extrinsic component, ≈ 0.6 eV, to heat the rest of the sorbent. For comparison, the thermodynamic minimum possible energy expenditure to separate CO_2 at 213 K is 0.16 eV per molecule [16].

Also shown in Fig. 2 are results where the criterion for $T_{\rm de}$ is maximum energy efficiency at each $T_{\rm ad}$, without regard to the length of time required for desorption. Under this criterion, $T_{\rm de}$ is lower and energy consumption is reduced by $0.1 - 0.2$ eV/CO_2.

$E_{\rm ad} \approx 0.4$ eV has been observed experimentally for TiO_2 [14], Fe_3O_4 [15], and Cr_2O_3 [22]. The expansion in the range of materials that could be applied is a potentially important advantage of operation in Antarctica: a reduction in the optimum binding energy from ≈ 0.55 eV at 25° C to ≈ 0.40 eV at $-60°$ C constitutes, by itself, only a $\approx 30\%$ energy saving, but, in addition to these oxides, it opens up a range of zeolite and metal-organic framework materials for consideration [10]. It may also allow opportunities for adsorption modulated not by temperature but by, for example, electric charge [23, 24].

5. Purging H_2O. During the Antarctice winter, the relative humidity is generally around 100% [25]. The adsorption energy of H_2O to a $TiO_2(110)$ surface is ≈ 0.9 eV, as compared with ≈ 0.4 eV for CO_2 [14]. Furthermore, except at cryogenic temperatures H_2O displaces adsorbed CO_2. If the sorbent material has similar binding energies for H_2O and CO_2 to $TiO_2(111)$, a water front, a dividing line between sites occupied with H_2O and sites occupied with CO_2, is expected to develop in the pores. If the desorption phase is not energetic enough to desorb H_2O, this front will move deeper into the pores with each adsorption/desorption cycle, until there are no

sites available for capture of CO_2.

The idea explored in this section is to periodically purge adsorbed H_2O with a very hot desorption phase. Taking E_{ad} for H_2O to be 0.9 eV, the desorption temperature is ≈ 800 K, constituting a temperature swing about 3.5 times larger than during a regular desorption cycle. Let N_{purge} be the purge period: every $N_{purge}{}^{th}$ cycle runs hot, at an energy cost of four times that of a regular desorption cycle. Between purge cycles, the number of binding sites occupied with H_2O and unavailable for CO_2 capture increases linearly: after n cycles, the fraction of binding sites occupied with H_2O is $n \times P_{H2O}/P_{CO2}$, where P_{H2O} is the vapour pressure of H_2O [26], and P_{CO2} that of CO_2. At an ambient pressure of 65 kPa, $P_{CO2} = 26$ Pa.

$N_{purge}(T_{ad})$ calculated within this model is shown in Fig. 3. N_{purge} at each T_{ad} is chosen to minimise the energy cost of the purge cycles per captured CO_2 molecule. For simplicity, this calculation was performed assuming a 100% occupation swing on the sites available for CO_2 capture.

At $-58°$ C, the H_2O purges add 85% to the energy consumption. Averaging over the temperature distribution below $-58°$ C, the purges add 39% to the energy consumption for heating the sorbent per captured CO_2 molecule. This energy cost is included in Table II.

Reducing the binding energy of H_2O would improve energy efficiency, but in contrast to operation in temperate climates, it is not necessary that the binding energy for H_2O be less than that of CO_2. Ref. [10] identifies compounds where the physisorption binding energy of H_2O may be comparable to that of CO_2, making them good candidates for operation in Antarctica. A two-stage capture process may also be possible, in which the first stage captures most of the incoming H_2O at a lower binding energy, reducing the frequency of purge cycles in the CO_2 stage.

6. The katabatic winds. Katabatic winds are drainage winds. The surface of the high plateau cools through radiation to space [27]. Air in contact with the surface cools, compresses, and flows downhill. The katabatic winds are an obvious potential power source because they are exceptionally strong and constant, and are strongest in winter, when the capture machinery operates. They are strongest around the perimeter of the ice sheet, so power would need to be transmitted to the high plateau where the capture machinery is sited. The katabatic winds hug the surface: the wind velocity is highest 100-200 m above the surface [28], matching the typical hub height of modern wind turbines.

How many turbines are required? The average winter wind speed 100 m above ground level exceeds 20 m/s over $1.5 \cdot 10^6$ km^2 of Antarctica [28]; turbines can be placed in these areas. Suppose an energy consumption of 2 eV per captured CO_2 molecule and operation for six months of the year. To capture 10 Gt CO_2/y, the power consumption is 3 TW during these six months. Set the rotor diameter to 100 m, and the mean turbine separation to 2 km; at this ratio of separation to rotor diameter the power generated by each turbine is $\approx 85\%$ of that generated by isolated turbines [29]. Set the air density to 1.3 kg/m^3, corresponding to an elevation of 1000 m and a temperature of $-25°$ C. With these parameters, each turbine generates ≈ 20 MW, and $\approx 1.5 \cdot 10^5$ turbines distributed over $\approx 5 \cdot 10^5$ km^2 are required. The power generated per unit land area is ≈ 6 W/m^2.

I conclude this section by noting that erection of an immense number of turbines around the perimeter of the east Antarctic ice sheet may offer a climactic benefit: if they slow the meridonal circulation over the ice sheet, the high plateau might cool further, allowing even more efficient capture and storage of CO_2.

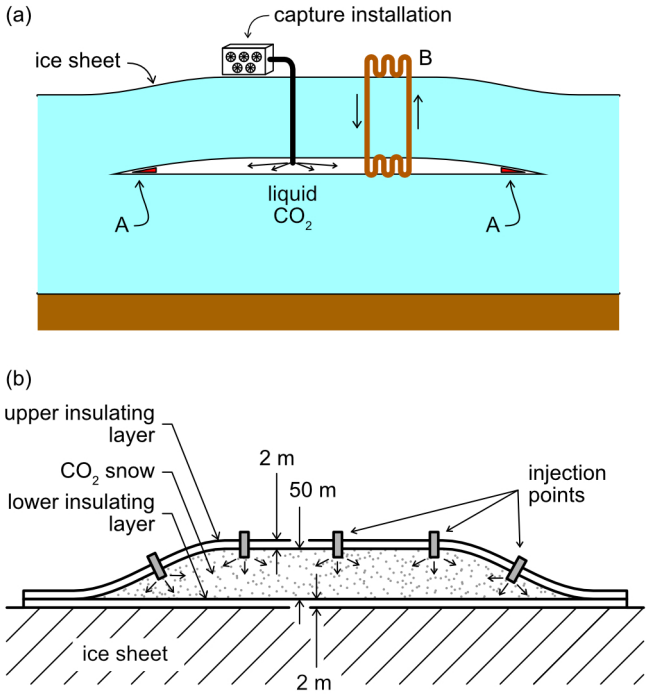

FIG. 4. (a) Storing the captured CO_2 by injecting it into the ice sheet. A: There might be machines that guide the opening of space for CO_2. B: The injected CO_2 could be solidified by circulating a working fluid when the surface temperature is below the triple point of CO_2, $-57°$ C. (b) Storing captured CO_2 as snow between insulating layers placed on the surface of the ice sheet.

7. Storage. Two possible storage schemes for the captured CO_2 are illustrated in Fig. 4. Panel (a) illustrates a scheme in which CO_2 is injected into the ice. Machines, labelled A in the figure, might guide the opening of the space for the CO_2, determining its depth below the surface. If it is ~ 1 km beneath the surface, then the ice sheet above will be lifted by CO_2 injected at a pressure of 10 MPa. 1000 m beneath the surface, the ice temperature is $\approx -47°$ C [32, 33]; at 10 MPa and $-47°$ C, CO_2 is

a liquid. To reduce the risk of seepage, after injection the CO_2 could be solidified by circulating a working fluid to the surface when the surface temperature is well below the triple point of CO_2, $-57°$ C. The CO_2 could also be injected as a slurry with water ice. 10 Gt/y of CO_2 corresponds to 6.3 km^3/y; if the CO_2 seam has an area of 10^4 km^2, the ice sheet gets lifted by 60 cm/y.

The energy required to compress CO_2 from 1.3 kPa to its triple point pressure, 515 kPa, is $\approx k_B T \log(515\text{ kPa}/1.3\text{ kPa}) \approx 0.1$ eV/molecule. Under an assumption of 50% efficiency, 0.2 eV per molecule is allocated for compression in Table II. Above 515 kPa, CO_2 is liquid, so the energy cost for further compression to 10 MPa is taken to be negligible. The energy required to open space in the ice sheet against a pressure of 10 MPa is well under 0.1 eV per molecule.

Fig. 4(b) illustrates a second possibility: storage of captured CO_2 as snow on the surface. CO_2 snow gets injected between insulating layers, and the upper layer rises as the CO_2 accumulates. Storage of CO_2 as snow on the Antarctic surface was proposed in Ref. [34]. If the density of the CO_2 snow is, like water snow at a depth of more than a few metres [30], around half the density of void-free solid CO_2, then to store 10 Gt/y at a layer thickness of 50 m, as indicated in the figure, requires 250 km^2/y. The vapour pressure of CO_2 reaches 65 kPa at $-83.8°$ C [31], 28 K below the annual mean temperature at the Vostok station [11]. Thermal insulation for buildings has a typical thermal conductivity of 0.04 W/m-K [35]. If the insulating layers are 2 m thick and have this thermal conductivity, the average heat flux is 1.1 W/m^2, or 280 MW for a year's worth of CO_2. The insulating layers could be provided with refigeration to counter this heat flow: it is a vastly smaller amount of energy than that required to capture the CO_2 in the first place. Should the refrigeration fail, the CO_2 layer would take about 700 years to sublimate.

8. Conclusion. Physisorption is widely regarded as impractical for direct air capture of CO_2 in temperate climates, due to the quantity of H_2O in the atmosphere. It may, however, be practical during the Antarctic winter. The much lower concentration of H_2O in the atmosphere and the lower binding energies required may open new routes for economical DAC on a gigatonne per year scale.

The author thanks M. Gunn, S. Simon, Y. Maeno, E. M. Forgan, J. C. Davis, and M. Freer for discussions.

APPENDIX

Here the pore dimensions are discussed further. The rate at which CO_2 is delivered to the inner lining of the sorbent tubes is given by:

$$R_{\mathrm{CO2}} \approx \frac{v \times \pi \left(d_{\mathrm{tube}}/2\right)^2 n_{\mathrm{CO2}}}{\pi d_{\mathrm{tube}} l_{\mathrm{tube}}} = \frac{v d_{\mathrm{tube}} n_{\mathrm{CO2}}}{4 l_{\mathrm{tube}}}.$$

n_{CO2} is the numerical concentration of CO_2 in the incoming air, which, at an air density of 1.1 kg/m^3, is $9.1 \cdot 10^{21}$ m^{-3}. R_{CO2} evaluates to $3.6 \cdot 10^{21}$ $m^{-2}s^{-1}$.

At short times, CO_2 diffuses into the pores faster than it can be delivered by the flow, and so the amount of CO_2 captured increases linearly in time. Supposing, for a moment, that the pores were infinitely long, there would eventually be a crossover to a diffusion-limited regime where the amount of CO_2 captured increases as $\sqrt{t}$. Let t_0 be the crossover time, and l_0 the depth that the CO_2 penetrates at time t_0. l_0 can be obtained from a condition that the flux due to diffusion, which is the diffusion constant D_{pore} multiplied by the concentration gradient, matches R_{CO2}:

$$R_{\mathrm{CO2}} = D_{\mathrm{pore}} \frac{n_{\mathrm{CO2}}}{l_0}. \tag{7}$$

In Fig. 1, $d_{\mathrm{pore}} = 40$ nm is indicated, which is less than the mean free path in air (65 nm at 293 K and 101 kPa [36]). Therefore it is reasonable to estimate D_{pore} in the molecular limit: $D_{\mathrm{pore}} \approx d_{\mathrm{pore}} v_z$, where v_z is the thermal velocity along the axis of the pore. $\frac{1}{2} m_{\mathrm{CO2}} v_z^2 = \frac{1}{2} k_B T$, where m_{CO2} is the mass of a CO_2 molecule, yielding $v_z = 200$ m/s at $T = 213$ K.

In the mass-transport-limited regime, the front of sites occupied with CO_2 moves inward at rate $R_{\mathrm{CO2}}/n_{\mathrm{sat,3D}}$, where $n_{\mathrm{sat,3D}}$ is the adsorption site density in m^{-3}. $n_{\mathrm{sat,3D}}$ is given by:

$$n_{\mathrm{sat,3D}} \approx n_{\mathrm{sat}} \times \pi d_{\mathrm{pore}} \times \frac{4}{\pi d_{\mathrm{pore}}^2} \equiv \frac{\beta}{d_{\mathrm{pore}}}.$$

Here, a constant β has been introduced, that, for $n_{\mathrm{sat}} = (4.3\text{ Å})^{-2}$, evaluates to $\beta = 2.2 \cdot 10^{19}$ m^{-2}. Taking l_0 from Eq. 7 and dividing by the velocity of the occupation front yields an expression for t_0:

$$t_0 = \frac{v_z n_{\mathrm{CO2}} \beta}{R_{\mathrm{CO2}}^2}. \tag{8}$$

t_0 evaluates to ≈ 3 s, independent of the pore diameter. For $d_{\mathrm{pore}} = 40$ nm, $l_0 \approx 20$ μm. l_{pore} is chosen to be a tenth of this to ensure rapid diffusion of CO_2 out of the pores during the desorption cycle.

* C.Hicks.1 (at) bham.ac.uk

[1] Ritchie, H., Roser, M. and Rosado, P., CO_2 and Greenhouse Gas Emissions. *Our World in Data.* (2020) https://ourworldindata.org/co2-and-other-greenhouse-gas-emissions

[2] IPCC, 2022: *Climate Change 2022: Impacts, Adaptation, and Vulnerability.* Contribution of Working Group II to the Sixth Assessment Report of the Intergovernmental Panel on Climate Change. Pörtner, H.-O., Roberts, D. C., Tignor, M.m Poloczanska, E. S., Mintenbeck, K., Alegría, A., Craig, M., Langsdorf, S., Löschke, S. Möller, V., Okem, A., and Rama, B. (eds.). Cambridge University Press. In press.

[3] McQueen, N., Vaz Gomes, K., McCormick, C., Blumanthal, K., Pisciotta, M., and Wilcox, J., A review of direct air capture (DAC): scaling up commercial technologies and innovating for the future. *Prog. Energy* **3**, 032001 (2021). DOI: 10.1088/2516-1083/abf1ce

[4] Beuttler, C., Charles, L., and Wurzbacher, J., The Role of Direct Air Capture in Mitigation of Anthropogenic Greenhouse Gas Emissions. *Front. Clim.* **1**, 10 (2019). DOI: 10.3389/fclim.2019.00010

[5] Keith, D. W., Holmes, G., St. Angelo, D., and Heidel, K., A Process for Capturing CO_2 from the Atmosphere. *Joule* **2**, 1573 (2018). DOI: 10.1016/j.joule.2018.05.006

[6] Wurzbacher, J. A., 2015. *Development of a temperature vacuum swing process for CO_2 capture from ambient air.* Ph. D. thesis, ETH Zürich, Zürich, Switzerland.

[7] Gebald, C., 2014. *Development of amine-functionalized adsorbent for carbon dioxide capture from atmospheric air.* Ph. D. thesis, ETH Zürich, Zürich, Switzerland.

[8] Knolle, J. M., Fayaz, M., and Sayari, A., Understanding the effect of water on CO_2 adsorption. *Chem. Rev.* **121**, 7280 (2021). DOI: 10.1021/acs.chemrev.0c00762

[9] Kumar, A., Madden, D. G., Lusi, M., Chen, K.-J., Daniels, E. A., Curtin, T., Perry, J. J. IV, and Zaworotko, M. J., Direct air capture of CO_2 by physisorbent materials. *Angew. Chem. Int. Ed.* **54**, 14372 (2015). DOI: 10.1002/anie.201506952

[10] Findley, J. M., and Sholl, D. S., Computational Screening of MOFs and Zeolites for Direct Air Capture of Carbon Dioxide under Humid Conditions. *J. Phys. Chem. C* textbf125, 24630 (2021). DOI: 10.1021/acs.jpcc.1c06924

[11] Turner, J., Lu, H., King, J., Marshall, G. J., Phillips, T., Bannister, D., and Colwell, S., Extreme temperatures in the Antarctic. *J. Climate* **34**, 2653 (2021). DOI: 10.1175/JCLI-D-20-0538.1

[12] `engineeringtoolbox.com`

[13] Moody, L. F., Friction factors for pipe flow. *Transac. A.S.M.E.* **66**, 671 (1944).

[14] Scott Smith, R., Li, Z., Chen, L., Dohnálek, Z., and Kay, B. D., Adsorption, Desorption, and Displacement Kinetics of H_2O and CO_2 on $TiO_2(110)$. *J. Phys. Chem. B* **118**, 8054 (2014). DOI: doi.org/10.1021/jp501131v

[15] Pavelec, J., Hulva, J., Halwidl, D., Bliem, R., Gamba, O., Jakub, Z., Brunbauer, F., Schmid, M., Diebold, U., and Parkinson, S., A multi-technique study of CO_2 adsorption on Fe_3O_4 magnetite. *J. Chem. Phys.* **146**, 014701 (2017). DOI: 10.1063/1.4973241

[16] Lackner, K. S., The thermodynamics of direct air capture of carbon dioxide. *Energy* **50**, 38 (2013). DOI: 10.1016/j.energy.2012.09.012

[17] Dohnálek, Z., Kim, J., Bondarchuk, O., White, J. M., and Kay, B. D., Physisorption of N_2, O_2, and CO on fully oxidized $TiO_2(110)$. *J. Phys. Chem. B* **110**, 6229 (2006). DOI: 10.1021/jp0564905

[18] McDonald, H. J., and Seltz, H., The Heat Capacities of Titanium Dioxide from 68-298°K. The Thermodynamic Properties of Titanium Dioxide. *J. Am. Chem. Soc.* **61**, 2405 (1939).

[19] Miao, Y., He, Z., Zhu, X., Izikowitz, D., and Li, J., Operating temperatures affect direct air capture of CO_2 in polyamine-loaded mesoporous silica. *Chemical Engineering Journal* **426**, 131875 (2021). DOI: 10.1016/j.cej.2021.131875

[20] Kumar, R., Bandyopadhyay, M., Pandey, M., Tsunoji, N., Amine-impregnated nanoarchitectonics of mesoporous silica for capturing dry and humid 400 ppm carbon dioxide: A comparative study. *Microporous and Mesoporous Materials* **338**, 111956 (2022). DOI: 10.1016/j.micromeso.2022.111956

[21] Varghese, A. M. and Karanikolos, G. N., CO_2 capture adsorbents functionalized by amine-bearing polymers: A review. *International Journal of Greenhouse Gas Control* **96**, 103005 (2020). DOI: 10.1016/j.ijggc.2020.103005

[22] Funk, S., Nurkic, T., Hokkanen, B., and Burghaus, U., CO_2 adsorption on Cr(110) and $Cr_2O_3(0001)/Cr(110)$. *Appl. Surf. Sci.* **253**, 7108 (2007). DOI: 10.1016/j.apsusc.2007.02.052

[23] Tao, L., Huang, J., Dastan, D., Wang, T., Lia, J, Yin, X., and Wang, Q., CO_2 capture and separation on charge-modulated calcite. *Appl. Surf. Sci.* **530**, 147265 (2020). DOI: 10.1016/j.apsusc.2020.147265

[24] Tan, X., Tahini, H. A., and Smith, S. C., Borophene as a promising material for charge-modulated switchable CO_2 capture. *Appl. Mater. Interfaces* **9**, 19825 (2017). DOI: 10.1021/acsami.7b03676

[25] Gettelman, A., Walden, V. P., Miloshevich, L. M., Roth, W. L., and Halter, B., Relative humidity over Antarctica from radiosondes, satellites, and a general circulation model. *J. Geophys. Research* **111**, D09S13 (2006). DOI: 10.1029/2005JD006636

[26] J. Marti and K. Mauersberger, A survey and new measurements of ice vapour pressure at temperatures between 170 and 250 K. *Geophysical Res. Lett.* **20**, 363 (1993). DOI: 10.1029/93GL00105

[27] T. A. Scambos, G. G. Campbell, A. Pope, T. Haran, A. Muto, M. Lazzara, C. H. Reijmer, and M. R. van den Broeke, Ultralow Surface Temperatures in East Antarctica From Satellite Thermal Infrared Mapping: The Coldest Places on Earth. *Geophysical Res. Lett.* **45**, 6124 (2018). DOI: 10.1029/2018GL078133

[28] Parish, T. R. and Bromwich, D. H., Reexamination of the near-surface airflow over the Antarctic continent and implications on atmospheric circulations at high southern latitudes. *Mon. Weather Rev.* **135**, 1961 (2007). DOI: 10.1175/MWR3374.1

[29] Meyers, J. and Meneveau, C., Optimal turbine spacing in fully developed wind farm boundary layers. *Wind Energy* **15**, 305 (2012). DOI: 10.1002/we.469

[30] Sturm, M., Taras, B., Liston, G. E., Derksen, C., Jonas, T., and Lea, J., Estimating snow water equivalent using snow depth data and climate classes. *J. Hydrometeorol.* **11**, 1380 (2010). DOI: 10.1175/2010JHM1202.1

[31] Meyers, C. H. and Van Dusen, M. S., The vapor pressure of liquid and solid carbon dioxide. *Bureau of Standards Journal of Research* **10**, 381 (1933).

[32] Price, P. B., Nagornov, O. V., Bay, R., Chirkin, D., He, Y., Miocinovic, P., Richards, A., Woschnagg, K., Koci, B., and Zagorodnov, V., Temperature profile for glacial ice at the South Pole: Implications for life in a nearby subglacial lake. *Proc. Nat. Acad. Sciences* **99**, 7844 (2002). DOI:10.1073.pnas.082238999

[33] Macelloni, G., Leduc-Leballeur, M., Montomoli, F., Brogioni, M., Ritz, C., and Picard, G., On the retrieval of internal temperature of Antarctica Ice Sheet by using SMOS observations. *Remote Sensing of Environment* **233**, 111405 (2019). DOI: 10.1016/j.rse.2019.111405

[34] Agee, E., Orton, A., and Rogers, J., CO_2 Snow Deposition in Antarctica to Curtail Anthropogenic Global Warming. *J. Appl. Meteorol. Climatol.* **52**, 281 (2013). DOI: 10.1175/JAMC-D-12-0110.1

[35] Asdrubali, F., D'Alessandro, F., and Schiavoni, S., A review of unconventional sustainable building insulation materials. *Sustainable Materials and Technologies* **4**, 1 (2015). DOI: 10.1016/j.susmat.2015.05.002.

[36] Jennings, S. G., The mean free path in air. *J. Aerosol. Sci.* **19**, 159 (1987). DOI: 10.1016/0021-8502(88)90219-4